International Journal of Non-Linear Mechanics 56 (2013) 25–33

Contents lists available at ScienceDirect

International Journal of Non-Linear Mechanics

journal homepage: www.elsevier.com/locate/nlm

Modeling and measuring visco-elastic properties: From collagen molecules to collagen fibrils

Alfonso Gautieri [a], Simone Vesentini [a], Alberto Redaelli [a], Roberto Ballarini [b,*]

[a] Biomechanics Group, Department of Electronics, Information and Bioengineering, Politecnico di Milano, Milan, Italy
[b] Department of Civil Engineering, University of Minnesota, 142 Civil Engineering Building, 500 Pillsbury Drive S.E., Minneapolis, MN 55455-0116, USA

ARTICLE INFO

Available online 2 April 2013

Keywords:
Collagen
Visco-elastic properties
Atomistic simulations
Micro-electro-mechanical systems
Biomechanics

ABSTRACT

Collagen is the main structural protein in vertebrate biology, determining the mechanical behavior of connective tissues such as tendon, bone and skin. Although extensive efforts in the study of the origin of collagen exceptional mechanical properties, a deep knowledge of the relationship between molecular structure and mechanical properties remains elusive, hindered by the complex hierarchical structure of collagen-based tissues. Understanding the viscoelastic behavior of collagenous tissues requires knowledge of the properties at each structural level. Whole tissues have been studied extensively, but less is known about the mechanical behavior at the submicron, fibrillar and molecular level. Hence, we investigate the viscoelastic properties at the molecular level by using an atomistic modeling approach, performing *in silico* creep tests of a collagen-like peptide. The results are compared with creep and relaxation tests at the level of isolated collagen fibrils performed previously using a micro-electro-mechanical systems platform. Individual collagen molecules present a non-linear viscoelastic behavior, with a Young's modulus increasing from 6 to 16 GPa (for strains up to 20%), a viscosity of 3.84 ± 0.38 Pa s, and a relaxation time in the range of 0.24–0.64 ns. At the fibrils level, stress–strain–time data indicate that isolated fibrils exhibit viscoelastic behavior that could be fitted using the Maxwell–Weichert model. The fibrils showed an elastic modulus of 123 ± 46 MPa. The time-dependent behavior was well fit using the two-time-constant Maxwell–Weichert model with a fast time response of 7 ± 2 s and a slow time response of 102 ± 5 s.

1. Introduction

The complex mechanical behavior observed in all connective tissues is directly related to their complex hierarchical structure and to their specific macromolecular components [1]. Theoretical prediction of the mechanical properties of soft tissues is notoriously difficult, being dependent on a detailed knowledge of their structure, as well as on the properties of the components and their interactions. Moreover such information is often unavailable and only phenomenological explanations of observed properties can be given. In general, the common methodology in bioengineering studies relies on a top-down approach, that is, measurements are gradually refined to be able to observe smaller structures and properties until technical limits are reached.

Mechanical investigations at higher hierarchical levels (*i.e.*, whole tissues and collagen fibers) have been performed for several decades. As a consequence, it is well known that collagen-rich tissue present viscoelastic behavior, as established from a larger number of creep and relaxation tests that have been performed on both tendons and ligaments [2–4]. Starting from the pioneering work of Fung [5], several constitutive and structural models have been developed to model the viscoelastic behavior of collagenous tissues [6–10]. Investigations at the fibril level have been performed through small angle X-ray scattering [11] to assess the fibril deformation inside tissue specimens. However, in this setup the load is not directly applied to single fibril and hence the response is averaged over several fibrils. Direct experiment on single fibrils are relatively recent and possible thanks to the use of atomic force microscopy and micro-mechanical systems (MEMS) which allowed the study of the elastic [12–16] and viscoelastic properties of collagen fibrils [17,18]. The experimental results performed using MEMS platforms and reported in numerous publications have been collected and are summarized in this paper so that they could be compared with the results of the models. Concerning the molecular level, although several studies have been performed using both experimental and computational procedures, the investigations focused solely on the elastic properties [19–27].

For this reasons, despite the abundant investigation of the viscoelastic behavior at the macro-scale and the very recent works on collagen fibril viscoelasticity, relatively little is known about the molecular and fibrillar origin of the time-dependent properties of

* Corresponding author. Tel.: +1 612 625 2148; fax: +1 612 626 7750.
E-mail address: broberto@umn.edu (R. Ballarini).

0020-7462/$ - see front matter © 2013 Elsevier Ltd. All rights reserved.
http://dx.doi.org/10.1016/j.ijnonlinmec.2013.03.012

collagenous tissues. It has been speculated that the elastic behavior of these tissues is due to the stretching of cross-linked collagen molecules and thus fibrils, whereas the energy dissipation (the viscous behavior) is thought to involve sliding of molecules and fibrils by each other during the tissue deformation [1,28]. However, there is still no clear understanding of the mechanisms behind the viscoelastic behavior of collagenous tissue, and on the role of each hierarchical scale in determining the overall mechanical properties. An important outstanding question is whether or not molecular-level load relaxation effects are important for the viscoelastic properties measured at larger scales. This paper describes the results of a combined computational and experimental study of the viscoelastic behavior of collagen molecules and collagen fibrils.

2. Molecular dynamics studies of single collagen molecules

An approach to investigate the molecular origin of collagen viscoelasticity, is the use of *in silico* tests to study collagen molecules from the level of amino acids upwards [29]. In this way it is possible to obtain quantitative data on the time-dependent mechanical behavior of single collagen molecules in order to assess molecular-level viscoelastic properties, and to scale up properties from there to larger tissue levels. In this approach, Steered Molecular Dynamics simulations are used to perform *in silico* creep tests (i.e., constant load tests) of collagen molecules, fitting the deformation response over time with a Kelvin–Voigt (KV) model. The KV model is a simple constitutive model consisting of a spring and a dashpot in parallel (see Fig. 1), where this approach allows us to compute the Young's modulus, the viscosity and the characteristic relaxation time of a single collagen molecule.

In order to perform constant force steered molecular dynamics (SMD) simulations, the three N-terminal C_α atoms are kept fixed whereas the three C-terminal C_α atoms are subject to an instantaneous constant force. This setup mimics a single molecule creep test, in which an instantaneous load is applied and the strain response in time is observed. The creep test simulations are run until asymptotic deformation and then strain–time curves obtained for collagen molecules during SMD simulations are fitted with the Kelvin–Voigt equation in order to estimate E (Young's modulus) and η (viscosity). The instantaneous stress σ_0 is calculated dividing the applied force by the cross-sectional area of collagen, assuming a round cross-section and a radius of 0.55 nm. The value of the radius is determined from dry collagenous tissue in which the lateral distance between molecules is found to be 1.1 nm [30].

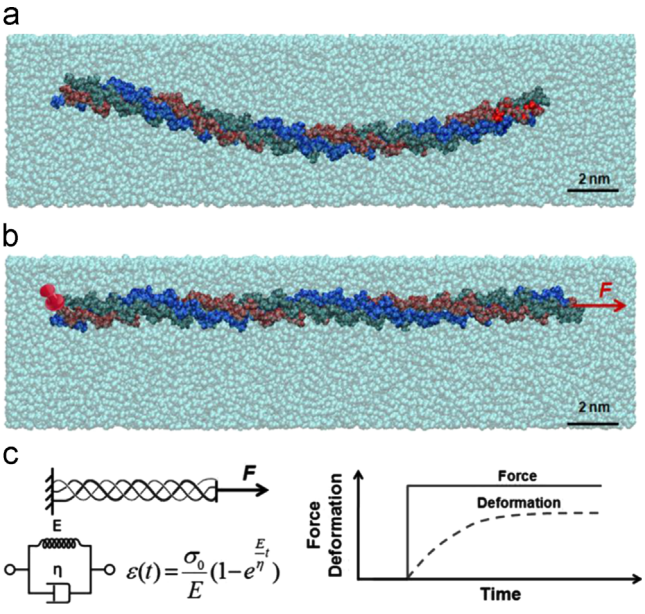

Fig. 1. Snapshots of the collagen peptide in water box. Panel a shows the conformation of the full atomistic model of a collagen peptide solvated in water box and equilibrated for 30 ns. After equilibration the molecule is subjected to virtual creep tests: one end of the collagen peptide is held fixed, whereas the other end is pulled with constant force (from 300 pN to 3,000 pN) until end-to-end distance reaches equilibrium (Panel b). Panel c shows a schematic of the creep test; a constant force is applied instantaneously to the molecule and its response (deformation over time) is monitored. The mechanical response of collagen molecule is modeled using a KV model, from which molecular Young's modulus (E) and viscosity (η) are calculated.

2.1. Viscoelasticity of solvated collagen molecules

When subjected to creep tests, the engineering strain of the molecule shows an exponential increase until asymptotic value is reached (see Fig. 2). This is the behavior typical of simple viscoelastic materials that can be characterized by a Young's modulus E, responsible for the elastic response, and a viscosity η, responsible for the viscous behavior. These results show that collagen molecule presents a non-linear elastic behavior, since the Young's modulus depends on the external load. In particular, for the loading conditions considered here E ranges from 6 to 16 GPa, a finding that matches several experimental [22,23,31,32] and modeling studies [27,33].

The collagen molecule viscosity has an average value of $3.84. \pm 0.38$ Pa s and it is not significantly affected by the external load. Based on the elastic modulus and the viscosity, the characteristic relaxation time (defined, for a KV model, as η/E) is calculated, obtaining values in the range 0.24–0.64 ns and 0.13–0.27 ns for solvated and dry molecule, respectively. Although the elastic behavior has been previously investigated, no experimental data is available for the viscous component of a single collagen molecule, although previous modeling studies from our group showed that the collagen molecule mechanical properties are rate-dependent [27]. This could be attributed to the very fast relaxation time (on the order of nanoseconds) of single molecules, which hinders its assessment using available experimental techniques. However, a recent work [34] demonstrated that Atomic Force Microscopy (AFM) can be successfully used to assess the viscoelastic properties of a single polypeptide chain, in this case polystyrene. According to this technique, referred to as “nanofishing” by the authors of that study, an AFM cantilever is mechanically oscillated at its resonant frequency during the stretching process. This enables the estimation of stiffness and viscosity of a single polymer chain with the use of a phenomenological model (the authors used a KV model). The polystyrene viscosity per unit length reported by the authors is 2.6×10^{-9} Kg/s, which resembles closely the findings for

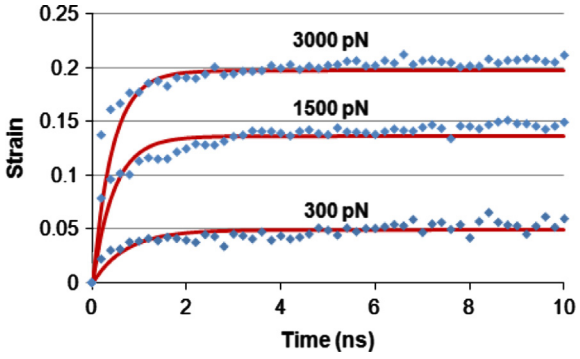

Fig. 2. Single molecule creep test. Mechanical response of solvated collagen molecule to creep tests for three cases with increasing value of external force. Dots represent the experimental data, whereas curves represent the fitted curves using a Kelvin–Voigt model.

collagen molecules, *i.e.*,$\approx 40\times 10^{-9}$ Kg/s (considering a peptide length of 20 nm). The slightly higher viscosity could be attributed to the fact that the polystyrene chain is a single strand, while the collagen peptide is in a triple helical configuration.

It is of great interest to discuss whether the two elements of the KV model, *i.e.* the purely elastic spring and the purely viscous dashpot, have an actual physical meaning. Similar efforts have been carried out in the recent modeling of the collagen fiber mechanical properties, in which the parameters in the proposed model were directly related to the composition of a collagen fiber [10]. For the present molecular model, a likely explanation would be that the elastic spring corresponds to the protein backbone, while the damping effect could be attributed to the interchain H-bonds. The backbone deformation include dihedral, angle and bond deformation, which are terms expressed by harmonic (or similar) functions in the molecular dynamics force field, and thus result in an elastic response to stretching. On the other hand, the viscous behavior may be due to the breaking and reforming of H-bonds, in particular H-bonds between the three collagen chains. Statistical mechanics based theories, and in particular Bell's model [35], has been applied to study the breaking of H-bonds (see, e.g. reference [36] and Fig. 3). It has been shown that the velocity at which a H-bond breaks is a function of the external force:

$$v = \frac{x_b}{\tau_0} e^{-[E_b - F x_b \cos\theta / k_b T]} \tag{1}$$

where v is the velocity at which the H-bond breaks, x_b is the distance between the equilibrium state and the transition state, τ_0 is the reciprocal of the bond natural frequency, E_b is the bond energy, F is the applied force, θ is the angle between the direction of the reaction pathway of bond breaking and the direction of applied load F, k_b is the Boltzmann constant and T is the temperature. The equation above shows that the mechanical response of the H-bonds is time-dependent, matching the behavior of the dashpot in the KV model very well (for which the stress is a function of the loading rate). Therefore the time-dependent rupture of H-bonds are likely responsible for the dissipative behavior observed in collagen molecule mechanics.

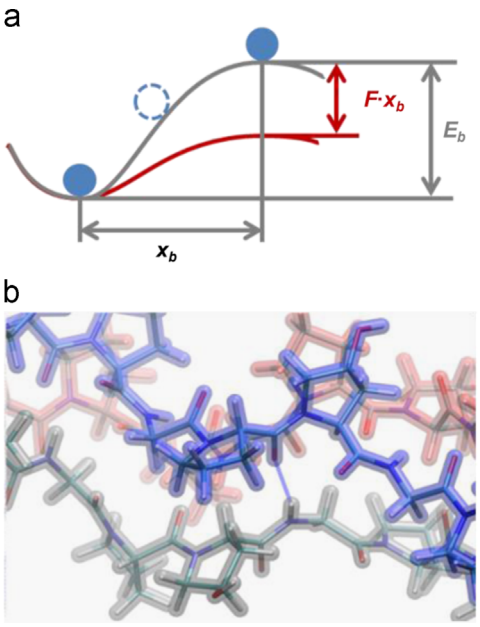

Fig. 3. Statistical theory to predict bond rupture mechanics. The graph depicts the energy as a function of a deformation variable (a), along a particular pathway that leads to bond rupture, where E_b is the energy barrier corresponding to the transition state. Panel b shows an interchain H-bond in collagen.

2.2. Comparison of molecular and fibrillar viscoelasticity

The systematic comparison of collagen molecule viscoelastic properties with those of the collagen fibrils yields two main observations:

1. The average Young's modulus decreases about six-fold from the single molecule level (≈6 GPa) [23,37] to the fibrillar scale (≈0.9 GPa) [11,12,14,15,17].
2. The viscosity of collagen molecules (3.84 Pa s, present work) is several orders of magnitude lower than the viscosity of fibrils (0.09–1.63 GPa s) (see Section 3). As a result, the characteristic relaxation time of the molecule (≈0.5 ns, given by η/E) is several orders of magnitude lower that the value found for the fibril (7–102 s, see Section 3).

In order to explain these observations, we attempt to upscale from a single molecule to fibril considering that collagen fibrils are assemblies of collagen molecules connected by covalent cross-links (see Fig. 4a) and arranged in a quasi-hexagonal array in cross-section [38] (Fig. 4b). Thus, the fibril can be modeled, in a first approximation, as a collection of KV elements arranged both in series and in parallel (Fig. 4c), where each of these elements account for a single collagen molecule.

We model the collagen molecule as a KV material, one of the simplest models for viscoelastic materials, which can be represented by an ideal viscous damper and an ideal elastic spring connected in parallel (see Fig. 1c). The KV model behavior can be expressed in terms of force and deformation:

$$\frac{F}{A} = \frac{kl}{A}\frac{\Delta l(t)}{l} + \eta\frac{\dot{\Delta} l(t)}{l} \tag{2}$$

$$\Delta l(t) = \frac{F}{k}(1 - e^{-(k/A/\eta/l)t}) \tag{3}$$

where F is the applied constant force, $\Delta l(t)$ is the deformation as a function of time t of the KV element of area A and length l, k is the spring elastic constant and η the viscosity of the damper. When N such elements are connected in series, the total deformation experienced by the system is the sum of the individual deformations.

Assuming that the N elements are identical (with the same spring constant k, viscosity η, area A and length l), the behavior of the system results:

$$\Delta l(t) = \frac{NF}{k}(1 - e^{-(k/A/\eta/l)t}) \tag{4}$$

Thus, when N identical KV elements are connected in series, the system itself behaves as a KV material with overall spring constant $k_{sys}=k/N$, whereas the characteristic time of the system remains the same as that of the unit elements. On the other hand, when N KV elements act in parallel, the total strain experienced by the system is the sum of the strain of each element.

Assuming that the N elements are identical (with the same spring constant k, viscosity η, area A and length l), the behavior of the system results:

$$\Delta l(t) = \frac{F}{Nk}(1 - e^{-(k/A/\eta/l)t}) \tag{5}$$

Thus, when N identical KV elements are connected in parallel, the system behaves as a KV material with overall spring constant $k_{sys}=kN$. Also in the parallel case, the characteristic time of the system is the same as that of the unit elements.

Within the fibril, collagen molecules are assembled in series staggered by a fixed period of about 67 nm (the so-called D-period). Laterally, the triple-helices are arranged in a quasi-hexagonal array in cross-section, with a lateral distance d (see Fig. 4b). Thus, in a fibril of cross-sectional area A_f, the number N_p of parallel molecules

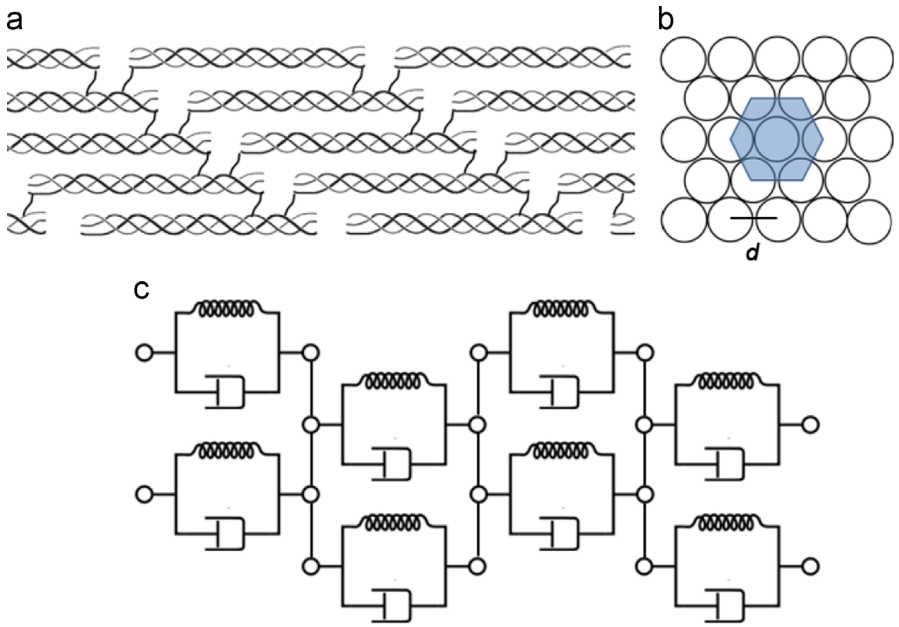

Fig. 4. Schematic of collagen fibril and viscoelastic model based on KV elements. Collagen type I form supramolecular structures, the collagen fibrils, where molecules are assembled in a staggered fashion by about 67 nm, *i.e.* the so-called D-period (Panel a). Laterally, the triple-helices are arranged in a quasi-hexagonal array in cross-section leading to fibril with diameters in the range 30–300 nm (Panel b). The molecular lateral distance d depends on the hydration states: the typical lateral spacing between molecules in the fibrils decreases from about 1.6 (hydrated state) to 1.1 nm (dry state) [30]. Within the fibril, collagen molecules are connected by covalent cross-links that ensure load transmission throughout the fibril structure. As a first approximation, the collagen fibril can be assumed as an assembly of multiple KV elements (each one representing a collagen molecule), connected both in series and in parallel (Panel c).

of area A_m results:

$$N_p = \frac{A_f \rho}{\pi (d/2)^2} \tag{6}$$

where ρ is the density of the hexagonal arrangement ($\rho \approx 0.9096$), *i.e.* the fraction of the plane occupied by identical circles hexagonally arranged. On the other hand, in a fibril of length L_f, the number N_s of serial molecules staggered by a distance s ($\approx$67 nm) results:

$$N_s = \frac{L_f}{s} \tag{7}$$

The fibril elastic constant k_f, considering N_p molecules acting in parallel and N_s molecules acting in series, results:

$$k_f = k_m \frac{N_p}{N_s} = \frac{E_m A_m}{L_m} \frac{A_f \rho}{\pi (d/2)^2} \frac{s}{L_f} \tag{8}$$

where k_m is the elastic constant of the single molecule and E_m its Young's modulus. Finally, the Young's modulus of the fibrils results:

$$E_f = k_f \frac{L_f}{A_f} = \frac{E_m A_m A_f \rho s}{L_m \pi (d/2)^2 L_f} \frac{L_f}{A_f} = \frac{E_m A_m \rho s}{L_m \pi (d/2)^2} \tag{9}$$

We can assume $E_m = 6$ GPa, $A_m = 9.5 \times 10^{-19}$ m^2 (given by a molecular radius of 0.55 nm), $\rho = 0.9096$, $s = 67$ nm and $L_m = 300$ nm. Concerning the value of the intermolecular lateral distance d, Fratzl et al. [30] found a lateral spacing of 1.6 nm for wet collagen. From Eq. (9) we obtain a Young's modulus of 0.57 GPa for wet collagen fibrils, a value that is in very good agreement with experimental and computational results ($\approx$0.8 GPa). Thus, it can be concluded that the elastic component of the fibril mechanical behavior is, in first approximation, well estimated assuming the fibril to be formed by a collection of KV elements (each representing a single collagen molecule) arranged in series (due to the D-periodic staggering, see Fig. 4a) and in parallel (due to the quasi-hexagonal packing, see Fig. 4b).

On the other hand, according to the model outlined above the characteristic time of such collection of KV elements is expected to be the same as that of the single KV element. In our case, however, we observe that the characteristic time of a collagen fibril (7–102 s) is several orders of magnitude higher than the value found here for the single collagen molecule ($\approx$0.5 ns). This implies that the viscous properties of collagen fibrils are not directly dictated by the single molecule behavior, but are largely dependent on other mechanisms, most likely the water-mediated shearing of the molecules within the fibril. This finding supports previous hypotheses based on mechanical tests on self-assembled collagen fibers [28]. In their work, the authors demonstrated a transition of collagen fiber mechanical properties from viscous to elastic depending on the cross-linking content, concluding that at low level of cross-linking the mechanical response is dominated by viscous sliding of collagen molecules and fibrils by each other, while at higher levels of cross-linking the mechanical response is mostly dictated by the elastic stretching of molecules.

3. Experimental creep and relaxation tests of isolated collagen fibrils

The mechanical testing of biological tissues at relatively large scales enjoys a long and rich history. However, data on the micro and nano scale features is sparse at best because of the difficulties associated with specimen preparation and handling and with the accurate measurement of forces and displacements. The mechanical properties of the larger features of bone, for example, have been studied using standard (albeit often customized) testing equipment, and more recently optical techniques have been applied to test the mechanical response of molecules. Until recently there was a void in experimentation of collagen fibrils and fibers because testing platforms were not available to measure forces and displacements to the appropriate dimensions. The void was partially filled by the development of microelectromechanical systems (MEMS) devices that produced first-time measurements of the strength, strain capacity, and viscoelastic properties of collagen fibrils subjected to simple elongation [14–16,18]. The MEMS platforms

enabled the measurement of the relaxation times of demineralized collagen fibrils, as described next.

The evolution and details of the MEMS technology used to design and fabricate the testing platforms, specimen preparation procedures, and structural testing protocols can be recovered from [14–16,18]. The first generation devices, which are not described in any detail here, used electrostatic actuation to apply force to the specimen, and the displacements were measured using a Vernier scale. The second generation devices rely on piezoelectric displacement transducers capable of applying displacement-controlled motions with nm-scale resolution. Digital-image-correlation software in conjunction with in-situ microscopy with digital image capture enabled displacement measurements in real-time at nm-scales. Representative data obtained from experiments using the two different devices is summarized in the next section. For both generation devices accurate determination of force from measured displacement was accomplished by using standard MEMS technology, as follows.

The basic idea of the MEMS paradigm is that if displacements of an elastic test structure with known dimensions and elastic moduli can be measured accurately, the forces can be determined using a structural analysis. One common material used to create MEMS devices is polycrystalline silicon. Standard MEMS processing techniques of deposition, patterning, and etching can produce polycrystalline silicon structures with dimensions ranging from sub-micrometer to hundreds of micrometers. The elastic properties of silicon are well-known but slightly anisotropic. Therefore the structural analyses of devices made from single-crystal silicon or large-grained polycrystalline silicon can be significantly more complicated than those performed for homogeneous isotropic structures. Fortunately, polycrystalline silicon deposited by chemical vapor deposition at temperatures below 600 °C contains grain sizes on the order of 100 nm [39]. Therefore, typical size MEMS devices will contain large numbers of silicon grains in all in-plane dimensions, leading to nearly isotropic in-plane elastic moduli [40].

The second generation device used most recently to test individual collagen fibrils [16,18] is shown schematically in Fig. 5. Multiple devices were fabricated with standard MEMS processing techniques, using 100 mm diameter silicon wafers as substrates. Using low-pressure chemical vapor deposition the wafers were sequentially coated with 3.5 μm of sacrificial silicon dioxide, and 6 μm of polycrystalline Si. The deposited layers were sufficiently annealed to relieve any growth-induced residual stresses. Devices were patterned using optical lithography, and then the polycrystalline silicon was etched in a sulfur hexafluoride plasma. The photoresist was removed in aqueous sulfuric acid and hydrogen peroxide, and devices were released by immersion in aqueous hydrofluoric acid, followed by rinsing in methanol and critical point carbon dioxide drying. The release etch dissolved all the sacrificial silicon dioxide beneath the portions of the device that were designed to be movable. The majority of the sacrificial silicon dioxide was left beneath areas of the device designed as anchors in order to keep the device attached to the silicon substrate. Because the device is less than 1 mm^2 in size, thousands of devices were fabricated simultaneously on a single silicon wafer.

With respect to the shematic shown in Fig. 5, the black areas labeled “A” are anchored to the substrate, while the gray areas are free to move. The device is designed for one end of the collagen fibril to be attached to the pad labeled “1” and the other end to be attached to the pad labeled “2”. A scanning electron microscope image of a representative device, upon which a collagen fibril is attached, is shown in Fig. 6. The central gray portion of the device is then attached to an external displacement transducer. In the work described in [16,18] this was achieved by placing a needle tip into the square hole created in the device and shown in the schematic and in the image, and by connecting the needle to a piezoelectric transducer-controlled stage. When the device is displaced to the left, as oriented in Fig. 5, the movement of all three positions, labeled “1”, “2”, and “3”, must be recorded simultaneously.

Since pad 1 is anchored to the substrate, the elongation of the collagen fibril specimen will be equal to the increase in separation between pads 1 and 2. The force applied to move pad 2 to the left is equal to the force applied to move pad 3 to the left. Therefore, the force applied to the specimen can be determined by measuring the elastic deformation involved in the increase in separation between pads 2 and 3. That separation is controlled by the elastic response of the polycrystalline silicon tether beams labeled “T” in Fig. 5. The dimensions of the tether beams can be measured very accurately using electron microscopy or other techniques, and the

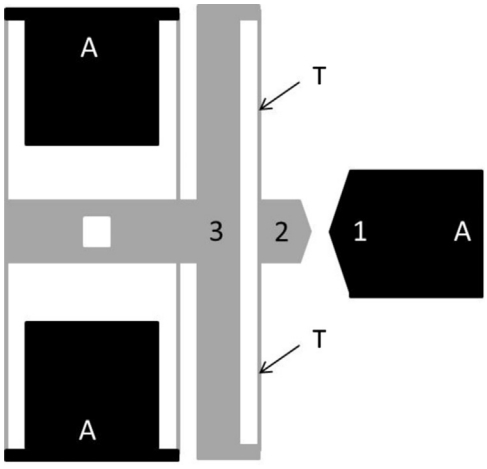

Fig. 5. Schematic of MEMS platform for testing collagen brils and other fiber-like structures.

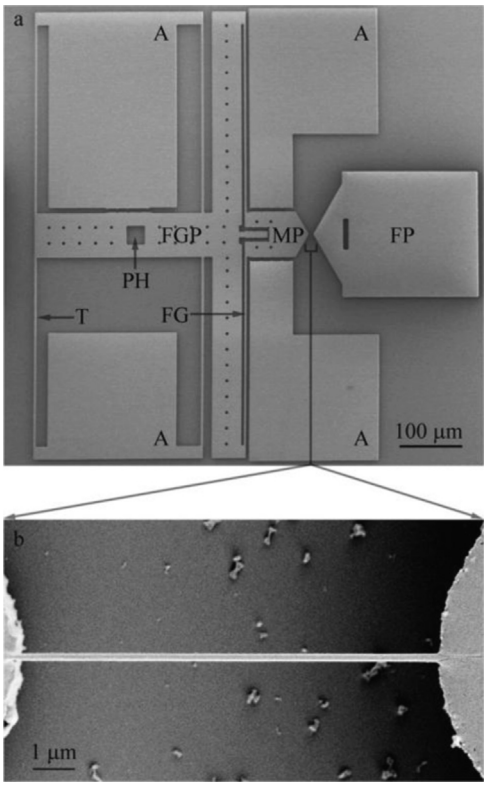

Fig. 6. MEMS platform for testing collagen fibrils [7,8].

elastic modulus of polycrystalline silicon is known [40,41]. This information can be used as input into a finite element model of the device to infer the forces necessary to achieve the observed displacements. In this manner, both the force and elongation of the fiber are determined simultaneously. Note that the range of available measurements will be optimized if the length, width and thickness of the tether beams are designed to have nearly the same stiffness as the nanoscale specimen. Materials with different stiffnesses can be tested by fabricating many devices with different tether beam stiffnesses on a single silicon wafer substrate, and then using whichever device best matches the material of interest.

The collagen fibrils studied using the first generation devices are considered as having been tested in air. This is because the testing machines involve an electrostatic actuator, and therefore could not be immersed in the liquid environment required to maintain the fibrils at 100% humidity throughout the test. Fibrils tested using these devices were pulled out of solution and kept in wet paper in an effort to minimize drying during the time required to attach them to the MEMS platforms and to perform the experiments. The second generation devices, however, enabled the fibrils to be maintained in a liquid environment provided by a liquid drop placed onto the MEMS platform for the duration of the experiment. Representative results are presented next that highlight the qualitative and quantitative response of individual collagen fibrils to three types of loading; monotonically increasing tension up to failure; loading to a fraction of the nominal strength followed by repeated unloading and reloading cycles; and creep-relaxation experiments.

3.1. Tensile strength and ultimate strain capacity

A representative nominal stress–nominal strain curve in the hydrated state reproduced from [16] is shown in Fig. 7. Note that the strain is averaged over the length of the fibril and is calculated as the stretch of the fibril divided by the original gage length. The stress, defined as the force divided by the average of cross-sectional area measurements imaged along a finite number of points along the fibril length, does not account for the significantly non-uniform cross-sectional area along the fibril and how it changes throughout the test. For these reasons the true stress and the maximum strain achieved at a particular point along the fibril are expected to be significantly higher than the nominal values. Fig. 7 shows that the response is linear and that the failure is brittle; there is no post-peak response for this nearly displacement controlled test. As expected the strength, strain capacity and elastic modulus data presented in [16] and reproduced in Table 1 showed significant specimen-to-specimen variation. It is remarkable that the fibrils are capable of stretching by as much as 180% and that their nominal strength can be as high as 0.5 GPa. The ability of the fibrils to sustain such large strains has never been reported; this result can be used to inform multiscale models of deformation and failure of collageneous tissues. The large batch-to-batch variation of the response in simple tension suggests that it will prove difficult to assess the validity of multiscale models of collagen fibrils.

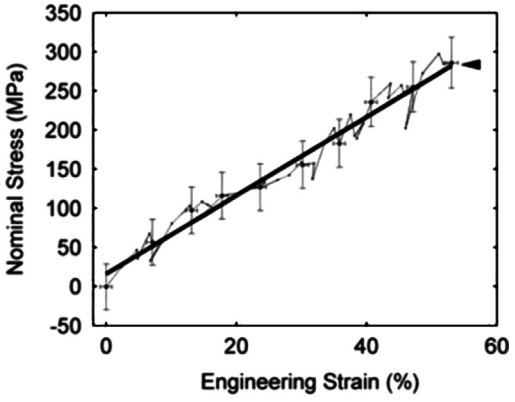

Fig. 7. Stress–strain curve of representative collagen fibril up to failure [7].

3.2. Initial evidence of viscoelasticity and strain recovery

The first generation MEMS platforms were used to study the response of collagen fibrils to loading/unloading cycles [14]. A representative cyclic stress–strain curve is shown in Fig. 8, where the unloading and subsequent reloading traces represent the average of the measurements over four cycles. The results show that collagen fibrils tested in air exhibit viscoelasticity and a residual strain upon removal of the load. But this is not the only rich constitutive behavior that was observed in the study reported in [14]. It was discovered that if a fibril is placed in a humid environment at the end of the cyclic loading experiment for a period of approximately one hour, the residual strain completely disappears. This is evidenced by Fig. 9, which shows the loading traces obtained from three tests on the same representative fibril discussed above (the top plot corresponds to Fig. 8). Each of the two additional tests was conducted after a one hour-long rest period. (Note that the unloading points were removed from the plots to render the Fig. less busy). It is observed that all stress–strain curves start at the origin, indicating complete strain recovery during the rest period and a modest reduction in stiffness. So in addition to time and possible rate effects, multiscale models must be challenged to account for the fibril's ability to recover strain when subjected to loading and unloading scenarios.

3.3. Creep-relaxation experiments and determination of relaxation times

The time effects observed in the initial experiments inspired the creep-relaxation tests described in [8]. Because of the mechanics of the test platform, the experiments cannot be performed under strictly constant force or constant displacement conditions. However, proper accounting of the force–displacement–time response

Table 1
Tensile properties of hydrated collagen fibrils [7].

	Strength (MPa)	Failure strain	Elastic modulus (MPa)
One standard deviation	230 ± 160	0.80 ± 0.44	470 ± 410
Range	40–490	0.33–1.83	110–1470

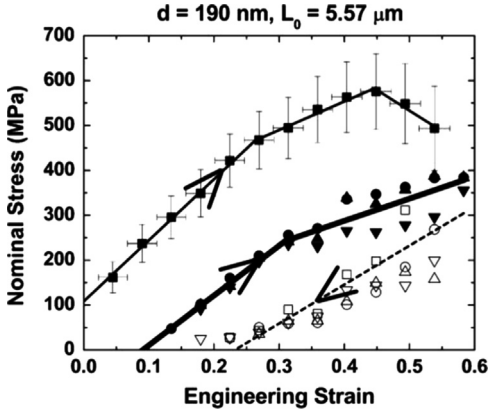

Fig. 8. Cyclic loading and unloading of a collagen fibril. The unloading and subsequent loading traces represent the average of four cycles [5].

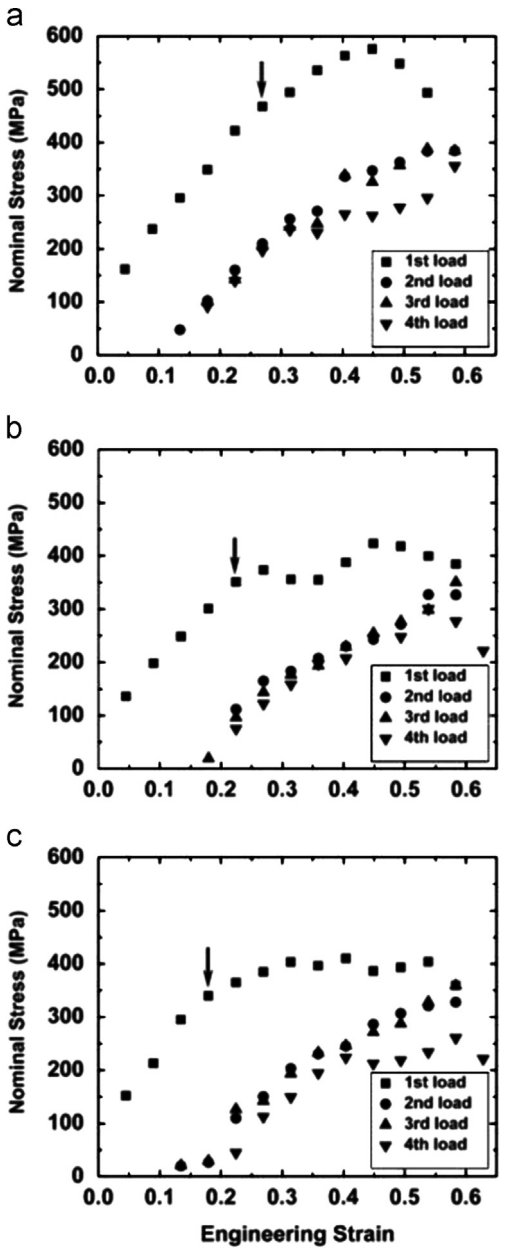

Fig. 9. Stress–strain curves produced by three tests on the same fibril with rest periods between the second and third experiments [5]. The unloading points were removed from the plots to render the figure less busy. The arrows indicate the point at which yielding appears to have initiated.

of the collagen fibrils produced the representative stress–time and strain–time plots shown in Fig. 10. This data was fitted well by the Maxwell–Weichert model illustrated in Fig. 11, which is associated with three elastic moduli and two viscous elements. The relaxation function associated with the Maxwell–Weicher model is given by

$$E_{relax}(t) = E_o + E_1 exp\left(-\frac{t}{\tau_1}\right) + E_2 exp\left(-\frac{t}{\tau_2}\right) \tag{10}$$

where E_o is the time-independent elastic modulus, and the relaxation time of each element, τ, is equal to the coefficient of viscosity of its dashpot, η, divided by the elastic modulus of its spring, E.

Fig. 12 shows typical fits of the relaxation modulus, and Fig. 13, reproduced from [18], lists the data derived from all the experiments. The results indicate that collagen fibrils have fast and slow time responses of the order of 10 and 100 s, respectively. The mechanism of viscoelasticity, discussed in much more detail in [18], was attributed to molecular rearrangement of collagen and water molecules; it is not dictated by the properties of the molecules, as suggested by the results of the previously discussed Kelvin–Voigt model of the fibril.

A comparison with other collagenous structures at larger scales (tissues) and smaller scales (collagen molecules) is warranted. Using Fung's QLV model [5,42], sheep flexor tendons were shown to have a short relaxation time of ~2 s and a long relaxation time of ~1500 s [43]. In a similar way, goat femur-medial-collateral-ligament-tibia complexes were shown to have a short relaxation time of ~2 s and a long relaxation time of ~2200 s [44]. Thus, compared to the long relaxation time of soft tissues (1500–2200 s), the long relaxation time of a single fibril is one order of magnitude smaller. The short relaxation time of the single isolated fibril is, conversely, three to four

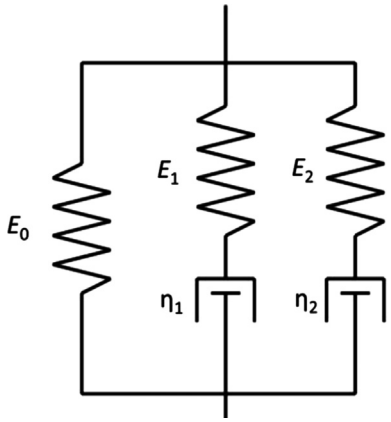

Fig. 11. Maxwell–Weichert model.

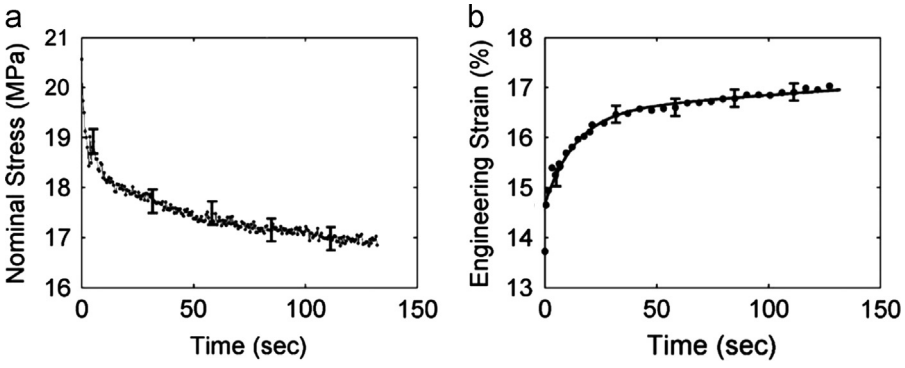

Fig. 10. Stress–time and strain–time data of representative collagen fibril [8].

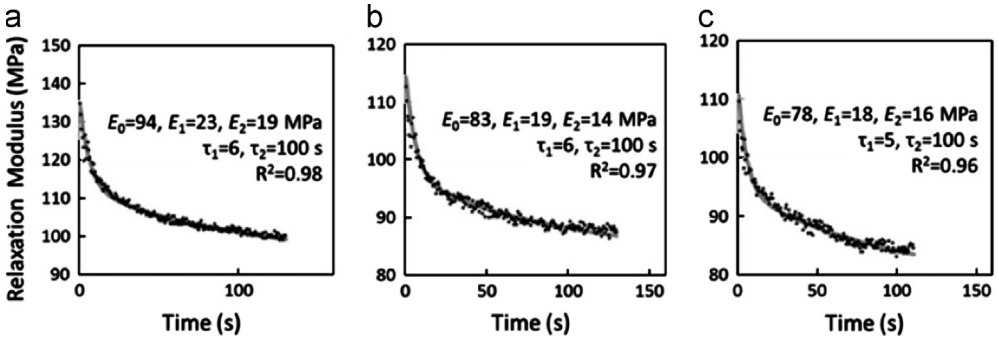

Fig. 12. Relaxation modulus of representative collagen fibril as derived using the Maxwell–Weichert model [8].

	E_0 (MPa)	E_1 (MPa)	E_2 (MPa)	τ_1 (s)	τ_2 (s)	R^2
Test 1 (N = 8)	140 ± 50 (80–250)	18 ± 4 (11–23)	20 ± 9 (8–35)	8.1 ± 2.0 (6–12)	100 ± 5 (100–110)	0.95 ± 0.03 (0.90–0.98)
Test 2 (N = 8)	120 ± 40 (70–210)	11 ± 6 (6–22)	13 ± 4 (7–17)	7.1 ± 3.2 (4–13)	100 ± 0 (100–100)	0.91 ± 0.05 (0.82–0.96)
Test 3 (N = 8)	110 ± 40 (60–190)	10 ± 4 (6–18)	13 ± 3 (8–18)	6.6 ± 1.3 (5–9)	100 ± 6 (90–110)	0.92 ± 0.05 (0.83–0.96)
Mean of all tests	123 ± 46	13 ± 6	16 ± 7	7 ± 2	102 ± 5	0.93 ± 0.04

Fig. 13. Parameters used to fit viscoelastic response of collagen fibrils using the Maxwell–Weichert model [8].

times longer than the bulk tissue. This is difficult to explain using first principles and may be an artifact of the phenomenological fitting. Another possibility is that the differences in time behavior arise from differences in tissue source. Given the data in hand at this point and assuming that model type and tissue source are not sufficient to explain an order-of-magnitude difference in relaxation time, the results suggest that the relaxation times of whole tissues are determined by components other than the collagen fibrils, most likely the ground substance (i.e., proteoglycans).

4. Conclusions

In this work, we performed *in silico* creep tests on collagen molecules and experimental MEMS testing on collagen fibrils to investigate the time-dependent mechanical properties of two important hierarchical scales within collagen complex structure.

From modeling stress–time curves we observe that collagen molecule behavior can be captured by a simple KV model (consisting in a spring and a dashpot in parallel), thus allowing us to determine single molecule viscoelastic properties. We find a nonlinear elastic component, with a Young's modulus ranging from 6 GPa to 16 GPa, in agreement with previous computational and experimental studies. The time-dependent properties show that collagen molecule has a viscosity of ≈4 Pa s and a relaxation time of ≈0.5 ns. From single molecule we upscale to the fibril, starting from the assumption that the fibril is formed by cross-linked collagen molecules and thus modeling the fibril as a collection of KV elements (each one accounting for one molecule) arranged in series an in parallel. Although this model is quite simplified, it allows us to give a good estimate of the elastic properties of the fibril starting from the Young's modulus of the single molecule. This suggests that the elastic component of fibril mechanical behavior is largely dictated by the stretching of triple helical molecules. On the other hand, this model fails to capture the time-dependence of fibril mechanical response, suggesting that the viscous component does not primarily depend on single molecule relaxation but largely relies on other mechanisms, such as water-mediated sliding of adjacent molecules.

Concerning the fibril level, we performed in vitro coupled creep and stress relaxation tests on type I collagen-fibril specimens using MEMS devices. The results suggest that isolated collagen fibrils are intrinsically viscoelastic. Using a simple Maxwell–Weichert model to fit the experimental data, we found a time independent elastic modulus of 140 ± 50 MPa upon initial loading to ~20% strain. Subsequent loads showed a drop to $\sim 115 \pm 41$ MPa. Time-dependent behavior was well fit using a two-time-constant model with a fast relaxation time of 7 ± 2 s and a long relaxation time of 102 ± 5 s. To our knowledge, this is the first time that the relaxation times of isolated collagen fibrils have been measured. The long relaxation time of isolated fibrils is an order of magnitude shorter than the long relaxation time of tendons and ligaments determined by Fung's QLV model. This is consistent with collagen fibrils contributing a fast viscoelastic behavior to collagenous tissues, with other tissue components providing the longer-duration viscous behavior.

Acknowledgment

We acknowledge support from Cariplo Foundation ("Advanced Materials"). High-performance computing resources have been provided by CINECA Consortium through the ISCRA initiative and by DEISA Consortium through the PRACE initiative.

References

[1] F.H. Silver, J.W. Freeman, I. Horvath, W.J. Landis, Molecular basis for elastic energy storage in mineralized tendon, Biomacromolecules 2 (2001) 750–756.
[2] X.T. Wang, R.F. Ker, Creep-rupture of wallaby tail tendons, Journal of Experimental Biology 198 (1995) 831–845.
[3] B.J. Rigby, N. Hirai, J.D. Spikes, H. Eyring, The mechanical properties of rat tail tendon, Journal of General Physiology 43 (1959) 265–283.
[4] N. Sasaki, N. Shukunami, N. Matsushima, Y. Izumi, Time-resolved X-ray diffraction from tendon collagen during creep using synchrotron radiation, Journal of Biomechanics 32 (1999) 285–292.
[5] Y.C. Fung, Elasticity of soft tissues in simple elongation, American Journal of Physiology 213 (1967) 1532–1544.
[6] R.C. Haut, R.W. Little, A constitutive equation for collagen fibers, Journal of Biomechanics 5 (1972) 423–430.
[7] J.M. Egan, A constitutive model for the mechanical behaviour of soft connective tissues, Journal of Biomechanics 20 (1987) 681–692.
[8] S.L.Y. Woo, G.A. Johnson, B.A. Smith, Mathematical-modeling of ligaments and tendons, Journal of Biomechanical Engineering-T Asme 115 (1993) 468–473.
[9] R. Puxkandl, I. Zizak, O. Paris, J. Keckes, W. Tesch, S. Bernstorff, P. Purslow, P. Fratzl, Viscoelastic properties of collagen: synchrotron radiation investigations and structural model, Philosophical Transactions of the Royal Society of London Series B-Biological Sciences 357 (2002) 191–197.
[10] R. Sopakayang, R. De Vita, A. Kwansa, J.W. Freeman, Elastic and viscoelastic properties of a type I collagen fiber, Journal of Theoretical Biology 293 (2012) 197–205.
[11] N. Sasaki, S. Odajima, Elongation mechanism of collagen fibrils and force–strain relations of tendon at each level of structural hierarchy, Journal of Biomechanics 29 (1996) 1131–1136.

[12] J.A.J. Van Der Rijt, K.O. Van Der Werf, M.L. Bennink, P.J. Dijkstra, J. Feijen, Micromechanical testing of individual collagen fibrils, Macromolecular Bioscience 6 (2006) 699–702.
[13] R.B. Svensson, T. Hassenkam, C.A. Grant, S.P. Magnusson, Tensile properties of human collagen fibrils and fascicles are insensitive to environmental salts, Biophysical Journal 99 (2010) 4020–4027.
[14] Z.L. Shen, M.R. Dodge, H. Kahn, R. Ballarini, S.J. Eppell, Stress–strain experiments on individual collagen fibrils, Biophysical Journal 95 (2008) 3956–3963.
[15] S.J. Eppell, B.N. Smith, H. Kahn, R. Ballarini, Nano measurements with microdevices: mechanical properties of hydrated collagen fibrils, Journal of the Royal Society Interface 3 (2006) 117–121.
[16] Z.L.L. Shen, M.R. Dodge, H. Kahn, R. Ballarini, S.J. Eppell, In vitro fracture testing of submicron diameter collagen fibril specimens, Biophysical Journal 99 (2010) 1986–1995.
[17] R.B. Svensson, T. Hassenkam, P. Hansen, S.P. Magnusson, Viscoelastic behavior of discrete human collagen fibrils, Journal of the Mechanical Behavior of Biomedical Materials 3 (2010) 112–115.
[18] Z.L. Shen, H. Kahn, R. Ballarini, S.J. Eppell, Viscoelastic properties of isolated collagen fibrils, Biophysical Journal 100 (2011) 3008–3015.
[19] R. Harley, D. James, A. Miller, J.W. White, Phonons and elastic-moduli of collagen and muscle, Nature 267 (1977) 285–287.
[20] S. Cusack, A. Miller, Determination of the elastic-constants of collagen by brillouin light-scattering, Journal of Molecular Biology 135 (1979) 39–51.
[21] H. Hofmann, T. Voss, K. Kuhn, J. Engel, Localization of flexible sites in thread-like molecules from electron-micrographs—comparison of interstitial, basement-membrane and intima collagens, Journal of Molecular Biology 172 (1984) 325–343.
[22] N. Sasaki, S. Odajima, Stress–strain curve and Young's modulus of a collagen molecule as determined by the X-ray diffraction technique, Journal of Biomechanics 29 (1996) 655–658.
[23] Y.L. Sun, Z.P. Luo, A. Fertala, K.N. An, Direct quantification of the flexibility of type I collagen monomer, Biochemical and Biophysical Research Communications 295 (2002) 382–386.
[24] M.J. Buehler, Atomistic and continuum modeling of mechanical properties of collagen: elasticity, fracture and self-assembly, Journal of Materials Research 21 (2006) 1947–1961.
[25] A. Gautieri, S. Vesentini, F.M. Montevecchi, A. Redaelli, Mechanical properties of physiological and pathological models of collagen peptides investigated via steered molecular dynamics simulations, Journal of Biomechanics 41 (2008) 3073–3077.
[26] A. Gautieri, A. Russo, S. Vesentini, A. Redaelli, M.J. Buehler, Coarse-grained model of collagen molecules using an extended MARTINI force field, Journal of Chemical Theory and Computation 6 (2010) 1210–1218.
[27] A. Gautieri, M.J. Buehler, A. Redaelli, Deformation rate controls elasticity and unfolding pathway of single tropocollagen molecules, Journal of the Mechanical Behavior of Biomedical Materials 2 (2009) 130–137.
[28] F.H. Silver, D.L. Christiansen, P.B. Snowhill, Y. Chen, Transition from viscous to elastic-based dependency of mechanical properties of self-assembled type I collagen fibers, Journal of Applied Polymer Science 79 (2001) 134–142.
[29] A. Gautieri, S. Vesentini, A. Redaelli, M.J. Buehler, Viscoelastic properties of model segments of collagen molecules, Matrix Biology 31 (2012) 141–149.
[30] P. Fratzl, N. Fratzlzelman, K. Klaushofer, Collagen packing and mineralization—an X-Ray-scattering investigation of turkey leg tendon, Biophysical Journal 64 (1993) 260–266.
[31] S. Cusack, A. Miller, Determination of the elastic constants of collagen by Brillouin light scattering, Journal of Molecular Biology 135 (1979) 39–51.
[32] R. Harley, D. James, A. Miller, J.W. White, Phonons and the elastic moduli of collagen and muscle, Nature 267 (1977) 285–287.
[33] M. Srinivasan, S.G.M. Uzel, A. Gautieri, S. Keten, M.J. Buehler, Alport Syndrome mutations in type IV tropocollagen alter molecular structure and nanomechanical properties, Journal of Structural Biology 168 (2009) 503–510.
[34] K. Nakajima, T. Nishi, Nanoscience of single polymer chains revealed by nanofishing, Chemical Record 6 (2006) 249–258.
[35] G.I. Bell, Theoretical-models for the specific adhesion of cells to cells or to surfaces, Advances in Applied Probability 12 (1980) 566–567.
[36] M.J. Buehler, T. Ackbarow, Fracture mechanics of protein materials, Materials Today 10 (2007) 46–58.
[37] Y.L. Sun, Z.P. Luo, A. Fertala, K.N. An, Stretching type II collagen with optical tweezers, Journal of Biomechanics 37 (2004) 1665–1669.
[38] J.P.R.O. Orgel, T.C. Irving, A. Miller, T.J. Wess, Microfibrillar structure of type I collagen in situ, Proceedings of the National Academy of Sciences USA 103 (2006) 9001–9005.
[39] H. Kahn, A.Q. He, A.H. Heuer, Homogeneous nucleation during crystallization of amorphous silicon produced by low-pressure chemical vapour deposition, Philosophical Magazine A 82 (2002) 137–165.
[40] R.L. Mullen, R. Ballarini, Y. Yin, A.H. Heuer, Monte Carlo simulation of effective elastic constants of polycrystalline thin films, Acta Materialia 45 (1997) 2247–2255.
[41] B.D. Jensen, M.P. de Boer, N.D. Masters, F. Bitsie, D.A. LaVan, Interferometry of actuated microcantilevers to determine material properties and test structure nonidealities in MEMS, Journal of Microelectromechanical Systems 10 (2001) 336–346.
[42] Y. Fung, N. Perrone, M. Anliker, Stress–Strain History Relations of Soft Tissues in Simple Elongation, Prentice-Hall, Englewood-Cliffs, New Jersey, 1972.
[43] J.J. Sarver, P.S. Robinson, D.M. Elliott, Methods for quasi-linear viscoelastic modeling of soft tissue: application to incremental stress-relaxation experiments, Journal of Biomechanical Engineering 125 (2003) 754–758.
[44] S.D. Abramowitch, S.L. Woo, An improved method to analyze the stress relaxation of ligaments following a finite ramp time based on the quasi-linear viscoelastic theory, Journal of Biomechanical Engineering 126 (2004) 92–97.